Available online at www.sciencedirect.com
SCIENCE DIRECT®
Journal of Solid State Chemistry 177 (2004) 2810–2817
JOURNAL OF SOLID STATE CHEMISTRY
http://elsevier.com/locate/jssc

Crystal structures of two new oxysulfides $La_5Ti_2MS_5O_7$ (M = Cu, Ag): evidence of anionic segregation

V. Meignen, L. Cario,* A. Lafond, Y. Moëlo, C. Guillot-Deudon, and A. Meerschaut

Laboratoire de Chimie des Solides, Institut des Matériaux Jean Rouxel, UMR 6502 CNRS-Université de Nantes, 2 rue de la Houssinière, BP 32229, 44 322 Nantes Cedex 03, France

Received 19 December 2003; received in revised form 2 April 2004; accepted 12 April 2004

Abstract

Two new compounds, $La_5Ti_2MS_5O_7$ (M = Cu, Ag) were synthesized and their structures solved from single crystal X-ray data. Both compounds are isotypic. They crystallize in the orthorhombic system (space group *Pnma*, $Z = 4$) with lattice constants $a = 19.423(1)$ Å, $b = 3.9793(2)$ Å, $c = 18.1191(9)$ Å for $La_5Ti_2CuS_5O_7$, and $a = 19.593(2)$ Å, $b = 3.9963(1)$ Å, and $c = 18.2973(15)$ Å for $La_5Ti_2AgS_5O_7$. The structure of these compounds is built from fragments of the rock-salt, perovskite and fluorite types and a clear anionic segregation of the anions appears in the structure. $La_5Ti_2CuS_5O_7$ and $La_5Ti_2AgS_5O_7$ exhibit an orange-yellow color and measurement of their optical band gap gave 2.02 and 2.17 eV, respectively.

Keywords: Oxysulfide; Rare earth; Crystal structure; Optical properties

1. Introduction

Recent explorations in the field of oxychalcogenides have revealed novel interesting layered intergrowth compounds with structures based on the stacking of chalcogenide and oxide layers. The $RE_2Ti_2S_2O_5$ (RE = La, Ce, Pr, Sm) compounds exhibit such intergrowth structures with $[RE_2S_2]$ rock-salt-type layers alternating regularly with $[Ti_2O_5]$ perovskite-type layers [1,2]. In the same way, the structure of the $(Sr_{n+1}M_nO_{3n-1})(Cu_2S_2)$ (M = Sc, Fe, Ni, Cu) compounds can be described as an intergrowth of $[Sr_{n+1}M_nO_{3n-1}]$ perovskite and $[Cu_2S_2]$ fluorite-type layers [3,4].

Since the combination of both oxide and chalcogenide layers often leads to materials with interesting physical properties (transparent conductors [5], photocatalyst materials [6], low-dimensional magnetism [7]), it seems of great interest to synthesize new layered oxychalcogenides. However, a good understanding of the factors governing the segregation in layers is still lacking. Looking at the reported structures which exhibit a segregation in oxide and chalcogenide layers reveals that they often contain electropositive elements, like rare-earth or alkaline-earth metals, combined with transition or post-transition metals. In these compounds the electropositive elements or the early transition elements can adopt mixed anion coordination while this is not true for late transition elements or post-transition elements. For instance, Ti is often found in mixed anion octahedra while Cu is always found in chalcogenide tetrahedra.

The presence of at least one cation like rare earth or Ti which can adopt mixed anion environment seems necessary to get a layered compound as it would insure the connection between the layers. However, the preference of late transition elements like Cu to be surrounded by only chalcogen atoms could reinforce the tendency towards segregation in layers of the structure. For these reasons we have started the investigation of the La–Ti–Cu–S–O and La–Ti–Ag–S–O systems in the hope to find new layered compounds.

This paper reports on the structure determination by means of single crystal X-ray crystallography of the first oxysulfides containing La, Ti and Cu/Ag. The structure

*Corresponding author. Fax: +02-40-37-39-95.
E-mail address: laurent.cario@cnrs-imn.fr (L. Cario).

0022-4596/$ - see front matter © 2004 Elsevier Inc. All rights reserved.
doi:10.1016/j.jssc.2004.04.023

of these compounds reveals a segregation of Cu/Ag in sulfide environment. However, the structure is not layered and it contains only fragments of layers. A more general discussion to understand the tendency towards anionic segregation shown by oxychalcogenide compounds is then presented.

2. Experimental

2.1. Synthesis and chemical analysis

$La_5Ti_2MS_5O_7$ (M = Cu, Ag) compounds were obtained from the reaction of La_2O_3, La_2S_3, TiO_2, and Cu_2S (or Ag_2S), in the ratio 1:3/2:2:1/2, in an evacuated silica tube. The initial mixture was heated at 1000°C during 1 week; an intermediate grinding and addition of iodine ($<5\,mg\,cm^{-3}$) were done before reheating at 1000°C, again for 1 week. This led to a crystallized powder of orange color corresponding to a mixture of the title compound (main phase) and of $La_2Ti_2O_7$ (impurity) (ICSD No. 72433). Chemical analysis was performed using an EDS-equipped scanning electron microscope. For the copper sample, part of the batch was included in epoxy (araldite type) and then polished. The averaged atomic percentages (excluding oxygen) obtained on 10 crystals are La 37.8(4)%, Cu 7.4(4)%, Ti 15.5(6)%, and S 39.3(8)%. The chemical analysis for the silver derivative was performed on powder. The averaged atomic percentages obtained on 12 spots are: La 37.7(1.0)%, Ti 15.4(5)%, Ag 7.8(8)% and S 39.2(1.3)%. These values are very close to the expected ones calculated according to the structural formula $La_5Ti_2MS_5O_7$ (La 38.46%, Ti 15.38%, M 7.69%, and S 38.46%).

2.2. Structure determination

Numerous small needle-shape single crystals of $La_5Ti_2CuS_5O_7$ were tested for crystallographic quality (intensity and shape of the spots). Despite our efforts they appeared of poor quality. Nevertheless, the best one was mounted on the Kappa CCD NONIUS diffractometer using Mo$K\alpha$ radiation ($\lambda = 0.71069$ Å). Operating conditions and X-ray crystallographic details are given in Table 1.

The crystal structure was solved by means of direct methods using the SHELXS programs [8]; refinement and subsequent difference-Fourier syntheses were performed with JANA2000 [9]. The systematic absences, $0\,k\,l$ with $k + l = 2n + 1$ and $h\,k\,0$ with $h = 2n + 1$, led to only two possible space groups, $Pn2_1a$ (No. 33,

Table 1
Crystal data and structure refinement for $La_5Ti_2CuS_5O_7$ and $La_5Ti_2AgS_5O_7$

Empirical formula	$La_5Ti_2CuS_5O_7$	$La_5Ti_2AgS_5O_7$
Formula weight ($g\,mol^{-1}$)	1126.1	1170.5
Temperature (K)	293(2)	293(2)
Wavelength (Å)	0.71069	0.71069
Crystal system	Orthorhombic	Orthorhombic
Space group	*Pnma*	*Pnma*
Unit cell dimensions (Å)	$a = 19.423(1)$	$a = 19.593(2)$
	$b = 3.9793(2)$	$b = 3.9963(1)$
	$c = 18.1191(9)$	$c = 18.2973(15)$
	33623 reflections used for the unit cell refinement	20651 reflections used for the unit cell refinement
Volume (Å^3)	1400.44(13)	1432.67(19)
Z	4	4
Density (calculated) ($mg\,m^{-3}$)	5.339	5.425
Absorption coefficient (mm^{-1})	18.22	17.69
Transmission min–max	0.242–0.874	0.501–0.877
$F(000)$	1976	2048
Crystal size (mm^3)	$0.215 \times 0.008 \times 0.008$	$0.08 \times 0.008 \times 0.008$
Theta range for data collection	3.07–35.02°	3.05–35°
Index ranges	$-27 \leqslant h \leqslant 31$, $-6 \leqslant k \leqslant 4$, $-27 \leqslant l \leqslant 28$	$-31 \leqslant h \leqslant 27$, $-6 \leqslant k \leqslant 6$, $-27 \leqslant l \leqslant 29$
Reflections collected	14285	19240
Independent reflections	2263 [R(int) for observed reflections = 0.070]	2334 [R(int) for observed reflections = 0.105]
Refinement method	Full-matrix least-squares on F^2	Full-matrix least-squares on F^2
Data/restraints/parameters	2263/0/101	2334/0/101
Goodness-of-fit on F^2	1.21	1.04
Refinement results	$R_{l_{obs}}/R_{l_{all}} = 0.0354/0.0723$	$R_{l_{obs}}/R_{l_{all}} = 0.0385/0.0922$
	$R_{w_{obs}}/R_{w_{all}} = 0.0412/0.0443$	$R_{w_{obs}}/R_{w_{all}} = 0.0387/0.0437$
	with 1585/2263 reflections	with 1480/2334 reflections
Residual electronic density ($e\,Å^{-3}$)	2.92 and −2.53	2.34 and −2.64

non-centrosymmetric, Calculated Figure Of Merit (CFOM) = 4.64) and *Pnma* (*no.* 62, centrosymmetric, CFOM = 1.54). The intensity statistics (mean $|E \times E - 1| = 0.919$) were in favor of a centrosymmetric space group, as well as the respective CFOM values. Therefore, we proceeded with the *Pnma* space group. Intensities were corrected for absorption effects using the faces indexed option (crystal bounded by faces {100}, {010}, and {001}, the longest dimension of the crystal corresponding to the *b*-axis, i.e., 3.9793 Å). In the final stages of refinement, i.e., with all atoms (except oxygen) refined anisotropically, the reliability factors converged to $R_{obs.} = 3.54\%$ and $R_w = 4.12\%$ for $N_{obs} = 1585$ reflections satisfying the criterion $I > 3\sigma(I)$ and 101 parameters ($R_{all} = 7.23\%$ for $N_{all} = 2263$ data); due to the poor quality of the crystal, the angular domain was restricted within the limits 3.07–30.0°. Fractional coordinates and equivalent atomic displacement parameters are given in Table 2; coefficients of the anisotropic displacement parameters for La, Cu, Ti, and S are given in Table 3.

The structure determination of $La_5AgTi_2S_5O_7$ was performed in the same way as for the copper compound (see Table 1 for details). The single crystals of the Ag-derivative were of very small sizes and poor quality. Fractional coordinates and equivalent atomic displacement parameters are given in Table 4; coefficients of the anisotropic displacement parameters for La, Ag, Ti, and S are given in Table 5.

2.3. Optical measurements

Optical measurements were performed with a Leitz spectrophotometer (MPV-SP), coupled with a metallographic microscope, working in the visible and close IR range (400–800 nm). For both compounds (Cu- and Ag-derivatives), the polarized transmitted light spectra were recorded on single crystals, with polarization directions perpendicular to the elongation of the crystals (*b*-axis).

3. Description of the crystal structure

Both compounds $La_5Ti_2MS_5O_7$ (M = Cu, Ag) are isostructural. Fig. 1a shows the crystal structure of $La_5Ti_2CuS_5O_7$ viewed down the *b*-axis and details the coordination polyhedra of each cation. In this figure, the labels of the different atoms correspond to those given in the asymmetric units of Table 3. The structure of $La_5Ti_2CuS_5O_7$ is not layered and seems rather complicated. However, as shown in Fig. 2 considering three different types of building blocks can ease the description. First, we consider a rock-salt-type fragment containing at each end side an interstitial Cu atom tetrahedrally coordinated by sulfur atoms (Fig. 2a). Then we note that a perovskite building block made of double chains of corner-sharing Ti-centered octahedra is present in the structure (Fig. 2b). Both building blocks together with the fluorite-type fragment shown in Fig. 2c condense to form a building unit shown in Fig. 2d. These building units periodically repeat in the structure as indicated in Fig. 2e.

As shown in Fig. 1b, La1 and La4 are located in bicapped trigonal prismatic environments (LaS_5O_3) while La2 and La3 atoms are found in tricapped trigonal prismatic environments (LaS_5O_4). On the other hand, La5 atoms are found in a seven-coordinate environment (LaO_5S_2) showing a rather complex

Table 2
Fractional coordinates and isotropic or equivalent atomic displacement parameters for $La_5Ti_2CuS_5O_7$

Atom	Site	x	y	z	U eq, iso* (Å^2)
La1	4*c*	0.69674(4)	0.75	0.28798(4)	0.0072(2)
La2	4*c*	0.51399(4)	0.75	0.37727(4)	0.0047(2)
La3	4*c*	0.31823(4)	0.75	0.47023(4)	0.0043(2)
La4	4*c*	0.10623(4)	0.75	0.50132(4)	0.0058(2)
La5	4*c*	0.54167(4)	0.25	0.19622(4)	0.0048(2)
Ti1	4*c*	0.19723(11)	0.25	0.38671(12)	0.0039(6)
Ti2	4*c*	0.37811(12)	0.25	0.32750(13)	0.0111(7)
Cu	4*c*	0.86009(9)	0.75	0.35199(10)	0.0153(5)
S1	4*c*	0.6301(2)	0.25	0.3803(2)	0.0050(8)
S2	4*c*	0.7795(2)	0.75	0.4550(2)	0.0070(9)
S3	4*c*	0.5679(2)	0.75	0.5337(2)	0.0071(9)
S4	4*c*	0.8255(2)	0.25	0.2912(2)	0.0084(9)
S5	4*c*	0.9701(2)	0.75	0.4067(2)	0.0070(8)
O1	4*c*	0.6761(4)	0.25	0.2093(5)	0.006(2)*
O2	4*c*	0.5748(4)	0.75	0.2546(4)	0.003(2)*
O3	4*c*	0.4711(4)	0.25	0.3055(4)	0.004(2)*
O4	4*c*	0.3801(4)	0.75	0.3431(5)	0.006(2)*
O5	4*c*	0.2956(4)	0.25	0.3910(5)	0.005(2)*
O6	4*c*	0.2002(4)	0.75	0.4029(5)	0.008(2)*
O7	4*c*	0.1064(4)	0.25	0.4237(4)	0.002(2)*

Table 3
Coefficients of the anisotropic displacement parameters (Å^2) for $La_5Ti_2CuS_5O_7$

Atom	U_{11}	U_{22}	U_{33}	U_{13}
La1	0.0068(3)	0.0024(3)	0.0123(4)	0.0006(3)
La2	0.0050(3)	0.0030(3)	0.0060(4)	0.0005(3)
La3	0.0056(3)	0.0024(3)	0.0049(4)	0.0000(3)
La4	0.0073(3)	0.0022(3)	0.0079(4)	0.0018(3)
La5	0.0068(3)	0.0026(3)	0.0050(4)	0.0009(3)
Ti1	0.0033(10)	0.0042(10)	0.0041(11)	0.0010(8)
Ti2	0.0033(11)	0.0242(13)	0.0059(12)	−0.0028(9)
Cu	0.0148(9)	0.0151(9)	0.0159(9)	−0.0035(7)
S1	0.0081(14)	0.0006(13)	0.0062(14)	0.0017(11)
S2	0.0057(14)	0.0023(14)	0.013(2)	0.0019(12)
S3	0.0073(15)	0.0077(14)	0.006(2)	−0.0039(12)
S4	0.0081(15)	0.0091(15)	0.0081(15)	0.0008(12)
S5	0.0065(14)	0.0055(14)	0.009(2)	0.0006(12)

$U_{12}=0$, $U_{23}=0$.

Table 4
Fractional coordinates and isotropic or equivalent atomic displacement parameters for $La_5Ti_2AgS_5O_7$

Atom	Site	x	y	z	U eq, iso* (Å^2)
La1	4c	0.69330(4)	0.75	0.28526(5)	0.0077(2)
La2	4c	0.51314(4)	0.75	0.37656(4)	0.0052(2)
La3	4c	0.31798(4)	0.75	0.47171(4)	0.0052(2)
La4	4c	0.10694(4)	0.75	0.50024(5)	0.0064(2)
La5	4c	0.54179(4)	0.25	0.19525(4)	0.0056(2)
Ti1	4c	0.19750(12)	0.25	0.38792(13)	0.0045(7)
Ti2	4c	0.37801(13)	0.25	0.33130(14)	0.0127(8)
Ag	4c	0.86628(6)	0.75	0.34386(7)	0.0207(4)
S1	4c	0.6286(2)	0.25	0.3793(2)	0.0079(10)
S2	4c	0.7791(2)	0.75	0.4567(2)	0.0092(10)
S3	4c	0.5675(2)	0.75	0.5335(2)	0.0072(10)
S4	4c	0.8165(2)	0.25	0.2801(2)	0.0097(10)
S5	4c	0.9752(2)	0.75	0.4109(2)	0.0083(10)
O1	4c	0.6724(5)	0.25	0.2078(5)	0.007(2)*
O2	4c	0.5725(5)	0.75	0.2540(5)	0.008(2)*
O3	4c	0.4695(4)	0.25	0.3056(5)	0.006(2)*
O4	4c	0.3811(4)	0.75	0.3453(5)	0.005(2)*
O5	4c	0.2950(4)	0.25	0.3939(5)	0.005(2)*
O6	4c	0.2017(5)	0.75	0.4027(5)	0.008(2)*
O7	4c	0.1068(4)	0.25	0.4244(5)	0.006(2)*

Table 5
Coefficients of the anisotropic displacement parameters (Å^2) for $La_5Ti_2AgS_5O_7$

Atom	U_{11}	U_{22}	U_{33}	U_{13}
La1	0.0049(4)	0.0045(4)	0.0139(4)	0.0013(3)
La2	0.0041(4)	0.0048(4)	0.0066(4)	0.0007(3)
La3	0.0053(4)	0.0036(4)	0.0067(4)	−0.0002(3)
La4	0.0063(4)	0.0041(4)	0.0087(4)	0.0023(3)
La5	0.0058(4)	0.0047(4)	0.0065(4)	0.0005(3)
Ti1	0.0018(12)	0.0057(12)	0.0060(12)	−0.0010(10)
Ti2	0.0024(13)	0.029(2)	0.0070(13)	0.0013(11)
Ag	0.0169(7)	0.0245(7)	0.0208(6)	−0.0078(6)
S1	0.006(2)	0.008(2)	0.009(2)	0.0020(14)
S2	0.008(2)	0.009(2)	0.010(2)	0.0002(14)
S3	0.006(2)	0.004(2)	0.012(2)	−0.0012(14)
S4	0.009(2)	0.008(2)	0.012(2)	0.0032(15)
S5	0.006(2)	0.008(2)	0.011(2)	0.0012(14)

$U_{12}=0$, $U_{23}=0$.

geometry. Both Ti atoms are octahedrally coordinated, with four O atoms forming the pseudo-equatorial plane. But the apical atoms differ for both Ti: one O and one S atom for Ti1 and two S atoms for Ti2. Four sulfur atoms coordinate the copper atom that is shifted from the center of the tetrahedra towards the triangular face. This shift is even more pronounced in the case of the silver compound.

Table 6 gathers the refined metal anion distances found in the structure of $La_5Ti_2CuS_5O_7$ and $La_5Ti_2AgS_5O_7$, and gives the bond valences calculated from these distances [10]. The metal anion distances are comparable with those found in related structures and bond valence calculations suggest the presence of La^{3+}, Cu^{+1}/Ag^{+1}, and Ti^{+4} ions. This is in good agreement with the oxidation state equilibrium reached for $La_5Ti_2MS_5O_7$ (M = Cu, Ag) by considering La(+III), M(+I) and Ti(+IV) counterbalancing S(−II) and O(−II).

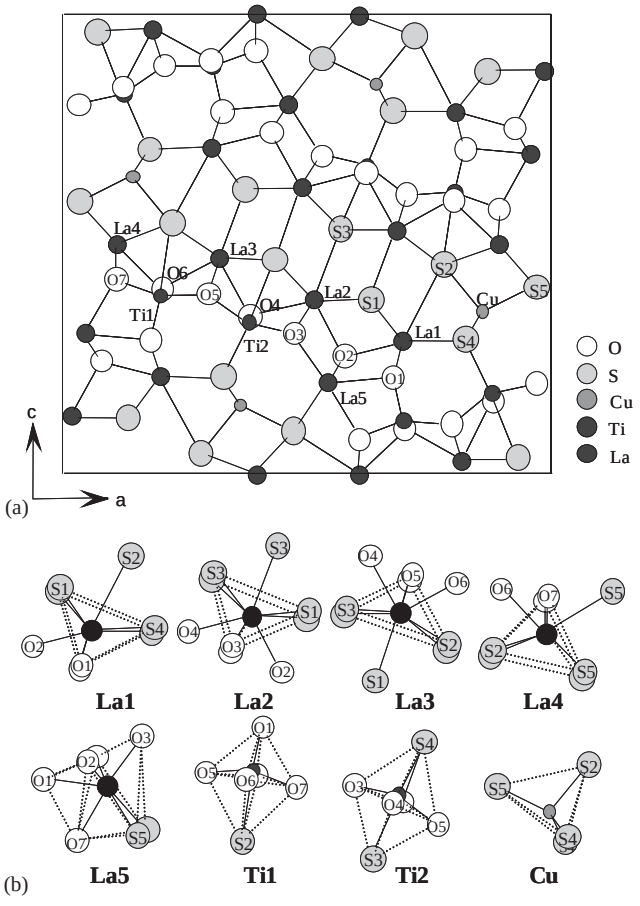

Fig. 1. Projection of the structure of $La_5Ti_2CuS_5O_7$ along the b-axis (a), and coordination polyhedrons surrounding each cation (b).

4. Diffuse reflectance measurements

Fig. 3 shows the absorption spectra of $La_5Ti_2MS_5O_7$ (M = Cu, Ag) obtained after a Kubelka–Munk transformation [11]. The crossing point between the baseline along the energy axis and the extrapolated line of the absorption edge gives the optical gap. For $La_5Ti_2CuS_5O_7$ and $La_5Ti_2AgS_5O_7$ the optical gaps are 2.02 and 2.17 eV, respectively. These gap values explain the yellow-orange color of both compounds and are close to those measured in the $Ln_2Ti_2S_2O_5$ series (2.05–2.14 eV with Ln from Nd to Er) [12]. It is worth noting that the Cu compound has a smaller gap than the Ag one, which is the opposite than the one observed for the pristine sulfides Cu_2S and Ag_2S 1.10 and 0.92 eV, respectively [13]. This discrepancy could be a consequence of the different coordination (2 or 3) and shorter Cu/Ag–S distances observed in the binaries (down to 2.227 Å for triangular Cu in Cu_2S; down to 2.430 Å for Ag in linear coordination in Ag_2S).

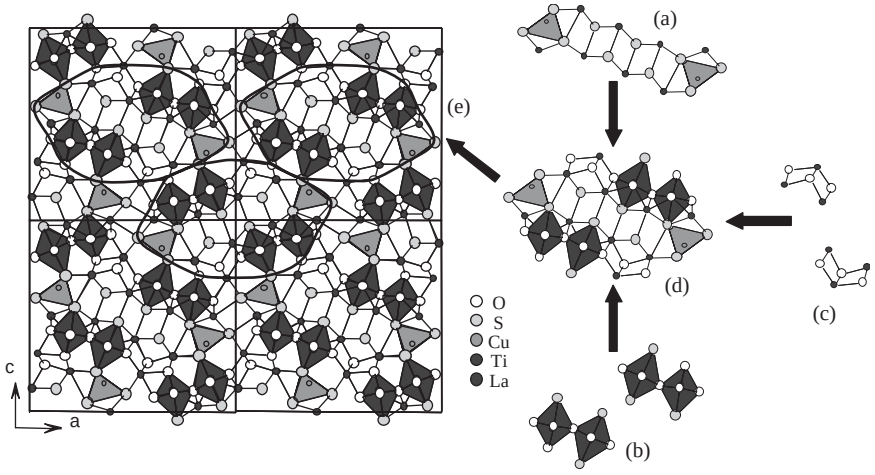

Fig. 2. Description of the structure of $La_5Ti_2CuS_5O_7$ from rock-salt (a), perovskite (b), and fluorite (c) type fragments. The packing of these fragments forms building units (d) that repeat regularly in the structure (e).

Table 6
Main interatomic bond lengths and calculated bond valence for $La_5Ti_2CuS_5O_7$ and $La_5Ti_2AgS_5O_7$

Bond	Sym. Op.[a]	$La_5Ti_2CuS_5O_7$		$La_5Ti_2AgS_5O_7$	
		Lengths (Å)	Bond valence	Lengths (Å)	Bond valence
La1–O2	#6	2.444(8)	0.479	2.435(9)	0.491
La1–O1 × 2	#6; #7	2.480(5)	2 × 0.435	2.484(5)	2 × 0.430
La1–S1 × 2	#1; #2	2.903(2)	2 × 0.491	2.925(3)	2 × 0.463
La1–S2	#2	3.426(3)	0.120	3.559(4)	0.083
La1–S4 × 2	#2; #3	3.196(3)	2 × 0.223	3.135(3)	2 × 0.262
			$\sum v = 2.90$		$\sum v = 2.88$
La2–O4	#12	2.673(9)	0.258	2.650(9)	0.275
La2–O2	#1	2.517(8)	0.394	2.526(9)	0.384
La2–O3 × 2	#12; #9	2.519(5)	2 × 0.391	2.532(5)	2 × 0.378
La2–S1 × 2	#7; #6	3.008(2)	2 × 0.370	3.019(3)	2 × 0.359
La2–S3 × 2	#1; #2	3.016(2)	2 × 0.362	3.033(3)	2 × 0.347
La2–S3	#6	3.022(3)	0.356	3.063(4)	0.319
			$\sum v = 3.26$		$\sum v = 3.15$
La3–O4	#12	2.598(8)	0.316	2.623(9)	0.296
La3–O6	#1	2.597(9)	0.317	2.604(9)	0.310
La3–O5 × 2	#9; #12	2.493(5)	2 × 0.420	2.495(5)	2 × 0.419
La3–S1	#1	2.888(3)	0.512	2.920(4)	0.469
La3–S2 × 2	#1; #2	3.065(2)	2 × 0.317	3.053(3)	2 × 0.328
La3–S3 × 2	#1; #2	2.975(2)	2 × 0.404	3.006(3)	2 × 0.372
			$\sum v = 3.43$		$\sum v = 3.31$
La4–O6	#1	2.552(9)	0.358	2.576(9)	0.336
La4–O7 × 2	#1; #2	2.437(5)	2 × 0.489	2.433(5)	2 × 0.494
La4–S2 × 2	#1; #2	3.085(2)	2 × 0.300	3.098(3)	2 × 0.290
La4–S5 × 2	#2; #11	2.989(2)	2 × 0.389	3.037(3)	2 × 0.342
La4–S5	#1	3.151(3)	0.251	3.054(3)	0.327
			$\sum v = 2.97$		$\sum v = 2.92$
La5–O2 × 2	#1; #2	2.343(4)	2 × 0.630	2.348(5)	2 × 0.623
La5–O1	#1	2.622(8)	0.296	2.569(9)	0.342
La5–O7	#4	2.511(8)	0.400	2.532(9)	0.377
La5–O3	#9	2.408(8)	0.528	2.466(9)	0.452
La5–S5 × 2	#9; #13	3.061(2)	2 × 0.321	3.077(3)	2 × 0.307
			$\sum v = 3.13$		$\sum v = 3.03$
Ti1–O6 × 2	#4; #5	2.012(1)	2 × 0.587	2.018(1)	2 × 0.578
Ti1–O1	#1	1.787(9)	1.079	1.818(9)	0.990
Ti1–O7	#4	1.887(8)	0.823	1.898(9)	0.800
Ti1–O5	#8	1.912(9)	0.769	1.914(9)	0.767
Ti1–S2	#4	2.904(4)	0.166	2.879(4)	0.178
			$\sum v = 4.01$		$\sum v = 3.89$
Ti2–O4 × 2	#2; #3	2.010(1)	2 × 0.590	2.015(1)	2 × 0.582
Ti2–O3	#2	1.850(8)	0.910	1.853(9)	0.902
Ti2–O5	#2	1.973(9)	0.652	1.989(9)	0.625
Ti2–S3	#10	2.725(4)	0.270	2.694(4)	0.293
Ti2–S4	#2	2.382(4)	0.681	2.368(4)	0.708
			$\sum v = 3.69$		$\sum v = 3.69$
M–S2	#2	2.436(4)	0.211	2.681(4)	0.238
M–S4 × 2	#2; #3	2.371(2)	2 × 0.251	2.511(2)	2 × 0.376
M–S5	#2	2.356(4)	0.262	2.463(4)	0.430
			$\sum v = 0.98$		$\sum v = 1.42$

[a] Symmetry operations: #1: x, y, z; #2: $x, 1+y, z$; #3: $x, 2+y, z$; #4: $-0.5+x, 0.5-y, 1.5-z$; #5: $-0.5+x, 1.5-y, 1.5-z$; #6: $1-x, 0.5+y, 1-z$; #7: $1-x, -0.5+y, 1-z$; #8: $1-x, 1.5+y, 1-z$; #9: $1.5-x, -y, 0.5+z$; #10: $1.5-x, -y, -0.5+z$; #11: $2-x, 0.5+y, 1-z$; #12: $1.5-x, -1-y, 0.5+z$; and #13: $1.5-x, 1-y, 0.5+z$.

5. Discussion and concluding remarks

The $La_5Ti_2MS_5O_7$ (M = Cu, Ag) compounds do not exhibit a layered structure. As already mentioned the structure contains only fragments of the rock-salt, perovskite and fluorite type. Many oxysulfides containing rare earth and a transition metal which have been reported, exhibit fragments or even layers of these types. In this respect, Fig. 4 shows the structure of $Sm_2Ti_2S_2O_5$ and $Pr_6Ti_2S_7O_6$ that exhibit a real similarity with $La_5Ti_2MS_5O_7$ (M = Cu, Ag). Indeed, $Sm_2Ti_2S_2O_5$ exhibits the simplest structure that is built up from a

stacking of rock-salt-type layer alternating with $[Ti_2O_5]$ perovskite-type layer. On the other hand, the recently reported structure of $Pr_6Ti_2S_7O_6$ [14] contains [*RE*S] planes that alternate with building units made of perovskite and rock-salt fragments. These building units resemble those found in the structure of $La_5Ti_2MS_5O_7$ (M = Cu, Ag) and shown in Fig. 2d.

Within these three compounds, Ti atoms are found in the same kind of fragments, namely a perovskite-type one, and they seem to be preferentially connected to oxygen atoms. On the other hand, the rare-earth atoms seem to be preferentially connected to sulfur atoms. This suggests that a kind of anionic segregation appears within these structures around each cation. In order to quantify such an anionic segregation the oxygen-bond-valence-ratio (OBVR) can be calculated according to the formula:

$$\mathrm{OBVR}(M) = \frac{\sum v_i(M-\mathrm{O})}{\sum v_i(M-\mathrm{O}) + \sum v_i(M-X)}$$

with v_i the bond valence, $M = RE$, Ti, X= S or Se, and with the summations running over all the metal–anion bonds in the unit cell. Fig. 5a shows the OBVR of *RE* and Ti versus the O/(O + S) ratio obtained for $La_5Ti_2CuS_5O_7$ and $La_5Ti_2AgS_5O_7$, and seven compounds reported in the *RE*–Ti–S–O quaternary system, including $Sm_2Ti_2S_2O_5$ and $Pr_6Ti_2S_7O_6$ [1,2,14–18]. In

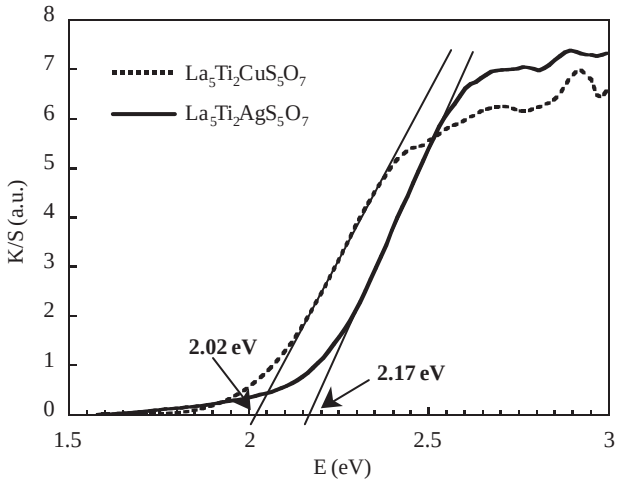

Fig. 3. Diffuse reflectance spectra of the $La_5Ti_2MS_5O_7$ (M = Cu,Ag) compounds obtained after a Kubelka–Munk transformation at room temperature.

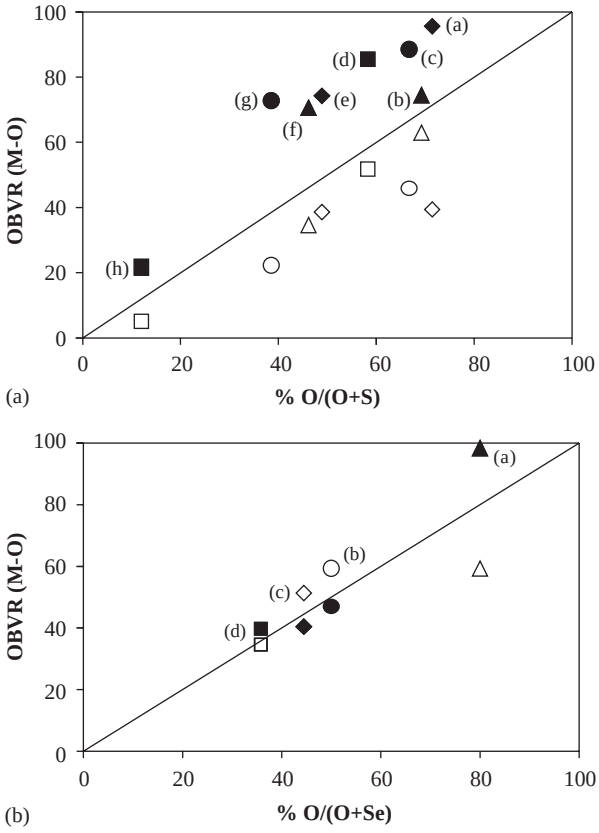

Fig. 5. OBVR of *RE* (open symbols) and Ti (full symbols) shown versus the O/(O + S) ratio. (1) OBVR calculated for $La_5Ti_2CuS_5O_7$ and seven compounds reported in the *RE*–Ti–S–O quaternary system: (a) $Sm_2Ti_2S_2O_5$ [1,2], (b) $Sm_2Ti_2S_2O_{4.5}$ [18], (c) $La_4Ti_3S_4O_8$ [15], (d) $La_5Ti_2CuS_5O_7$, (e) $La_{16}Ti_5S_{17.75}O_{17}$ [16], (f) $Pr_6Ti_2S_7O_6$ [14], (g) $La_6Ti_2S_8O_5$ [15], and (h) $La_{20}Ti_{11}S_{44}O_6$ [17]. (2) OBVR calculated for four compounds reported in the *RE*–Ti–Se–O quaternary system (a) $Sm_3Ti_3Se_2O_8$ [19], (b) $Gd_4TiSe_4O_4$ [20], (c) $La_4Ti_2Se_5O_4$ [21], and (d) $La_6Ti_3Se_9O_5$ [21].

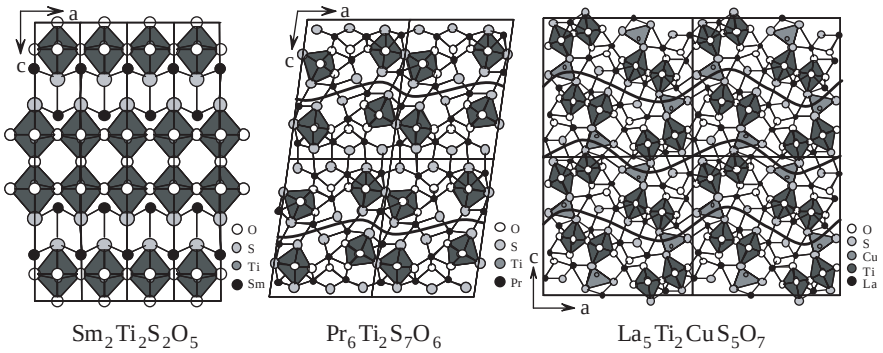

Fig. 4. Comparison of the structures of $Sm_2Ti_2S_2O_5$ and $Pr_6Ti_2S_7O_6$ with the structure of $La_5Ti_2CuS_5O_7$. All these structures are built from rock-salt and perovskite-type fragments or layers.

this figure, the straight line indicates the theoretical case in which the valence exchange with oxygen would correspond to the anionic ratio O/(O + S).

It appears that for all these different structures, the OBVR of Ti atoms is above the straight line while that of *RE* is found below. This clearly attests to an anionic segregation in the *RE*–Ti–S–O system with Ti preferentially connected to oxygen atoms and *RE* preferentially connected to sulfur atoms. As expected, the OBVR of Ti and *RE* roughly increases with the O/(O + S) ratio. For structures with close values of the O/(O + S) ratio, the difference between the OBVR of Ti and *RE* (Δ(OBV-R) = OBVR (Ti)–OBVR(*RE*)) is a good indication of the anionic segregation. We note that the oxidation state of Ti plays a major role in the anionic segregation. For example, $Sm_2Ti_2S_2O_5$ that contains Ti^{4+}, and $Sm_2Ti_2S_2O_{4.5}$ that contains Ti in a mixed valence state [18] have very close formulations and O/(O + S) ratios but show very different OBVR for Ti and Δ(OBVR). In the same way, considering different couple of anions, e.g., oxyselenide instead of oxysulfide, leads to a different situation for the anionic segregation. Fig. 5b shows the OBVR of *RE* and Ti calculated for the four known structures in the *RE*–Ti–Se–O system [19–21]. In this case, there is no obvious trend concerning the anionic segregation with sometimes Δ(OBVR) negative or positive.

The OBVR calculation on the *RE* and Ti oxysulfides quantifies the anionic segregation. Ti atoms always share a higher bond valence fraction with oxygen than with sulfur. It is the contrary for *RE* atoms. The same anionic segregation is observed for $La_5Ti_2CuS_5O_7$ and $La_5Ti_2AgS_5O_7$ with Ti in oxygen-rich environment and Cu or Ag in sulfur-rich environment. Despite this anionic segregation, that we were expecting, the structure is not segregated in layers. However, it is made of fragments of layers that appear frequently for the *RE* and Ti oxysulfides family.

References

[1] C. Boyer, C. Deudon, A. Meerschaut, C.R. Acad. Sci. 2 (Série IIc) (1999) 93–99 (Paris).
[2] M. Goga, R. Seshadri, V. Ksenofontov, P. Gütlich, W. Tremel, Chem. Commun. (1999) 979–980.
[3] W.J. Zhu, P.H. Hor, J. Solid State Chem. 134 (1997) 128–131.
[4] K. Otzschi, H. Ogino, J.I. Shimoyama, K. Kishio, J. Low Temp. Phys. 117 (1999) 729–733.
[5] K. Ueda, S. Inoue, S. Hirose, H. Kawazoe, H. Hosono, Appl. Phys. Lett. 78 (2001) 2333.
[6] A. Ishikawa, T. Takata, J.N. Kondo, M. Hara, H. Kobayashi, K. Domen, J. Am. Chem. Soc. 124 (2002) 13547–13553.
[7] (a) Y. Takano, T. Tsubaki, C. Itoi, K. Takase, K. Sekizawa, Solid State Commun. 122 (2002) 661–664;
(b) S. Okada, M. Matoba, H. Yoshida, K. Ohoyama, Y. Yamaguchi, J. Phys. Chem. Solids 63 (2002) 983–985.
[8] G.M. Sheldrick, SHELXL-97, Crystal Structure Refinement, UNIX version, Release 97-2, 1997.
[9] V. Petricek, M. Dusek, JANA2000: crystallographic computing system, version 14/06/02, Institute of Physics, Academy of Sciences of the Czech Republic, Praha.
[10] (a) N.E. Brese, M. O'Keeffe, Acta Crystallogr. B 47 (1991) 192–197;
(b) I.D. Brown, in: M. O'Keeffe, A. Navrostsky (Ed.), The Bond Valence Method, Structure and Bondings in Crystals, Vol. II, Academic Press, New York, 1981.
[11] W.W. Wendlandt, H.G. Hecht, Reflectance Spectroscopy, Intersciences, New York, 1966.
[12] C. Boyer-Candalen, J. Derouet, P. Porcher, Y. Moëlo, A. Meerschaut, J. Solid State Chem. 165 (2002) 228–237.
[13] S.I. Boldish, B.E. White, Am. Miner. 83 (1998) 865–871.
[14] A.S. Gardberg, J.A. Ibers, Z. Kristallogr. NCS 216 (2001) 491–492.
[15] J.A. Cody, J.A. Ibers, J. Solid State Chem. 114 (1995) 406–412.
[16] V. Meignen, A. Lafond, L. Cario, C. Deudon, A. Meerschaut, Acta Crystallogr. C 59 (2003) i63–i64.
[17] C. Deudon, A. Meerschaut, L. Cario, J. Rouxel, J. Solid State Chem. 120 (1995) 164–169.
[18] C. Guillot-Deudon, V. Meignen, A. Lafond, A. Meerschaut, J. Solid State Chem. (2004), in preparation.
[19] V. Meignen, C. Deudon, A. Lafond, C. Boyer, A. Meerschaut, Solid State Sciences 3 (2001) 189–194.
[20] A. Meerschaut, A. Lafond, V. Meignen, C. Deudon, J. Solid State Chem. 162 (2001) 182–187.
[21] O. Tougait, J.A. Ibers, J. Solid State Chem. 157 (2001) 289–295.